

Distribution Agreement

In presenting this thesis as a partial fulfillment of the requirements for a degree from Emory University, I hereby grant to Emory University and its agents the non-exclusive license to archive, make accessible, and display my thesis in whole or in part in all forms of media, now or hereafter now, including display on the World Wide Web. I understand that I may select some access restrictions as part of the online submission of this thesis. I retain all ownership rights to the copyright of the thesis. I also retain the right to use in future works (such as articles or books) all or part of this thesis.

Regina Luu

April 13, 2020

Salt Effects on Peptide-Phosphate Co-Assemblies

by

Regina Luu

David Lynn
Adviser

Department of Chemistry

David Lynn
Adviser

Eri Saikawa
Committee Member

Simba Nkomo
Committee Member

2021

Salt Effects on Peptide-Phosphate Co-Assemblies

By

Regina Luu

David Lynn

Adviser

An abstract of
a thesis submitted to the Faculty of Emory College of Arts and Sciences
of Emory University in partial fulfillment
of the requirements of the degree of
Bachelor of Science with Honors

Department of Chemistry

2021

Abstract

Salt Effects on Peptide-Phosphate Co-Assemblies

By Regina Luu

Short peptide chains have promiscuous binding abilities and unique assembly with themselves as well as phosphate template molecules, with one of the most known being DNA. Additionally, liquid-liquid phase separation helps give rise to nanostructures, such as nanotubes, specific to the templates that peptides are arrayed across. To further extend the knowledge around conditions that facilitate and promote the formation of nanotubes, we aimed to study the effects of various salt ions on the peptide-phosphate co-assemblies. Residual salts from synthesis and purification of peptides have been shown to be sufficient in destabilizing co-assembly nanotubes as observed as quick transitions to other nanostructures like ribbons, sheets, or fibers. Treatment of the salted peptide co-assemblies in increasingly concentrated NaCl solution also correlated with the transitions in the morphology away from nanotubes. In addition, examining the effects of the iodide and lithium ions in comparison to NaCl showed that co-assembly nanotubes were reduced in number and had generated thinner nanotube walls. Moreover, peptide co-assemblies with single-stranded DNA compared to double-stranded DNA under increased salt concentrations showed that greater β -sheet character is observed when the template is double-stranded DNA. Meanwhile, we observed that lithium ions can be capable of inducing a conformational DNA change from B to A form to create kinetically stabilized β -sheets observable through the ThT fluorescence assay. Uncovering the fundamentals behind co-assembly stabilization has applications in understanding the behavior of Nature's biopolymers in the context of neurodegenerative diseases like Alzheimer's disease and provides the basis for rational design of bio-inspired materials.

Salt Effects on Peptide-Phosphate Co-Assemblies

By

Regina Luu

David Lynn

Adviser

A thesis submitted to the Faculty of Emory College of Arts and Sciences
of Emory University in partial fulfillment
of the requirements of the degree of
Bachelor of Science with Honors

Department of Chemistry

2021

Acknowledgements

I would like to thank my research advisor Dr. David Lynn for all support that I have received which has furthered my passion for science and research. I am thankful for all the thought-provoking questions and his willingness to sit down and brainstorm solutions and future possibilities with me.

I would also like to thank my committee members Dr. Eri Saikawa and Dr. Simba Nkomo for their full support and commitment in advancing my thesis project. I greatly appreciate the all the thoughtful insights and comments that I have received.

I would especially like to thank all the past and current members of the Lynn lab who have been a major source of support and encouragement without which I would not have been able to complete my project: Dr. Anthony Sementilli, Youngsun Kim, Christella Dhammaputri, Ayanna Jones, Alexis Blake, Jipeng Yue, Nicolas Ingle, Seth Young, Griffin Davis, and Abhi Mudigonda. Being surrounded by all these wonderful people has made my research experience incredibly fulfilling and enjoyable. Finally, I would like to express additional acknowledgment for Christella who has been the most outstanding mentor that I could have ever asked for.

Table of Contents

| | |
|---|----|
| Introduction | 1 |
| Results and Discussion | 4 |
| <i>Co-assembly with Trimetaphosphate</i> | 4 |
| Figure 1. | 4 |
| Figure 2. | 5 |
| <i>Pep-KG:TMP Co-assembly Structural Stability</i> | 5 |
| Figure 2. | 5 |
| Figure 3. | 6 |
| Figure 4. | 7 |
| Figure 5. | 10 |
| Figure 6. | 12 |
| Figure 7. | 13 |
| <i>Pep-KG: DNA-Salt Effects on DNA Conformation</i> | 14 |
| Figure 8. | 15 |
| Figure 9. | 15 |
| Figure 10. | 16 |
| Conclusion | 17 |
| Materials and Methods | 18 |
| <i>Peptide synthesis and purification</i> | 18 |
| <i>Desalting peptides</i> | 19 |
| <i>Peptide assembly and peptide:phosphate co-assemblies</i> | 19 |
| <i>Transmission electron microscopy (TEM)</i> | 19 |
| <i>Circular dichroism (CD)</i> | 20 |
| <i>Thioflavin (ThT) fluorescence assay</i> | 20 |

Introduction

The structure-function paradigm, wherein the function of proteins will only be realized upon folding, was generally thought as a biological universal rule, reinforced by Christian Anfinsen's classic RNase A experiment. This experiment demonstrated that, by not allowing a previously denatured RNase A to re-fold into its native structure, the enzyme would lose its function and become “inactive,” thus supporting the notion that a protein’s activity depends upon its 3-D structure.¹ However, there exists a class of proteins which instead lack well-defined secondary structural characteristics under physiological conditions yet still retain function. They are called intrinsically disordered proteins (IDPs) and are known to be much more highly conserved in eukaryotic organisms compared to prokaryotes, and they fulfill critical roles in signal transduction², genomic circuits², and organelle assembly³. Although generally known as “disordered proteins,” IDPs are comprised of domains that are both ordered and disordered. Like other polymeric materials, IDPs benefit from their rapidly interchangeable balance of defined structures along with the promiscuous nature of their disordered states.

For instance, IDPs can have multiple functions due to their ability to have high specificity with respect to binding partners whilst maintaining relatively low affinity for those said binding partners.² IDP high binding specificity is achieved through chain flexibility that can conform to complementarity binding interfaces of their targets.² As the folding of an IDP raises its free energy the coupled binding of this folded IDP with a partner lowers the free energy so the resulting net free energy change is less than that of a pure binding event.² The consequence of smaller net free-energy change from coupled folding and binding is lowered binding affinity.² This is especially useful in terms of signal transduction as IDPs are capable of kinetically rapid association times as shown in the protein-protein interaction of the intrinsically disordered domain of cMyb to the transcription factor co-activator CBP’s KIX domain.⁴ Another key characteristic of IDPs is their unusually low hydrophobicity content with many IDPs containing a high charged amino acid content instead.² This hydrophobicity difference prevents IDPs from collapsing in biological conditions like well-folded globular proteins. In fact, highly charged proteins often experience strong electrostatic repulsion within the polypeptide which causes the IDP to unfold/expand rather than collapse when at a low ionic strength.⁵ Yet, in the presence of an ionic

denaturant (guanidinium chloride) and above the salt's critical concentration, the charged residues are screened, allowing for the IDP to collapse.⁵ It is now known that electrostatic interactions as well as sequence effects have a role in determining the structural integrity of IDPs. This behavior is also reminiscent of coacervate phase behavior, which describes a liquid-liquid phase separation between two oppositely charged polymers.^{6,7}

Liquid-liquid phase separation allows for higher-order assemblies, such as the formation of membraneless organelles. This phenomenon is most well studied in the case of ribosomal sub compartment formation and self-assembly. Being the center of protein assembly, the ribosome is strategically separated by membraneless compartments embedded in one another so that different chemical processes can occur in distinct physiological conditions isolated from one another.^{3,8} The beginning of the self-assembly process is marked by the formation of ribonucleoprotein complexes through interactions of intrinsically disordered proteins and ribosomal DNA which is driven by electrostatic interactions between these oppositely charged polyelectrolytes.⁹ These dynamic complexes become concentrated enough to face undergo liquid-liquid phase separation (LLPS) from the surrounding solution. The ribosomal solution continues to differentiate into three phase separated layers: the fibrillar center (FC), the dense fibrillar component (DFC), and the granular component (GC).³ Each of these layers forms through differences in the bulk surface tension in these otherwise coexisting stable liquid phases.³ Akin to an assembly line, the separation between these three liquid-like phases promotes directed processing of precursor ribosomal RNA through each successive phase in a distinct order.³ This demonstrates the ability of LLPS in spatially and temporally organizing cellular components that is encoded in of the inherent disorder of these biopolymers.

Therefore, it should come as no surprise that the presence and concentrations of various ions can have an important role to play in controlling phase behaviors. Salt ions have a contribution to the electrostatics that drive the phase separation during complex coacervation. There is a favorable increase in entropy of counter ions as the interaction between polymer-ions decrease and then are replaced by polymer-polymer interactions.¹⁰ Experimentally lowering the salt concentration has been often shown

to promote LLPS, which suggests the electrostatics as a dominating force for IDP systems in which this phenomenon occurs.¹⁰⁻¹²

IDPs are known to associate and consequently organize into distinct macromolecular structures through intermolecular interactions between identified motifs. The collapse from disordered-ness to a more stable conformation is facilitated by conformational sampling, in which the less ordered IDPs undergo various conformational changes but will select a specific conformation that is most stable at the time, often as a result of selection by various binding partners.¹³ An infamous IDP associated with Alzheimer's Disease pathology, containing an essential nucleating core sequence, 16KLVFFA, that is known to organize into a cross- β assembly *in vitro*, which can adopt either parallel or anti-parallel β -sheets and stack upon another via backbone H-bonding.¹⁴ These peptide assemblies can create higher-order structures such as nanoribbons, fibers, and nanotubes.¹⁵ An A β 42 congener, Ac-KLVIIAG-NH₂ or Pep-KG, assembles into fibers on its own but forms nanotubes in the presence of anionic polymers, such as polyphosphate or oligonucleotides through charge passivation of the positively charged Lys residue.¹⁴

Other A β congeners, Ac-KLVFFAE-NH₂ (E22, wildtype) and Ac-KLVFFAQ-NH₂ (E22Q), have been discovered to undergo a two-step nucleation that takes advantage of a transition through a metastable particle phase.¹⁶ This particle phase was probed through spectroscopic structural analyses which include fluorescence and electron microscopy that provided imaging of the particle phase whilst IR and NMR studies were used to investigate the physical characteristics of β -sheets assemblies.¹⁶ The proposed two-step nucleation model occurs through LLPS, beginning with protein-protein interactions creating a solute-rich internal environment that hosts different protein conformations within a constrained area.¹⁶ The elongation process proceeds with variations in the stacking and sampling of different β -sheets that result in a variety of final morphologies where the most stable one is selected for.

As a proof of concept, the co-assembly of various amyloid peptides and nucleic acids has been shown to produce multilamellar nanotubes.¹⁴ Not only does altering the sequence of the amyloid peptide make way for slight changes in the external surface but using other charged template molecules besides nucleic acids yields distinct structures and outputs. To make full use out of the nature of amyloid

peptides and their template-based conformational changes, the present paper presents an investigation into how different phosphate-based molecules and changing salt concentrations affect the co-assembly of intrinsically disordered peptides and template polymers.

Results and Discussion

Co-assembly with Trimetaphosphate

Previous research has shown that the peptide Ac-KLVIIAG-NH₂ or Pep-KG, when incubated with nucleic acid strands, co-assembles to form nanotubes that are driven by electrostatic complementarity (**Figure 1**).¹⁴ As this has been established, we sought to investigate the properties underlying the electrostatic interaction by instead co-assembling with sodium trimetaphosphate (TMP) as it is simpler polymeric anion structure while maintaining the electrostatically attraction to Pep-KG (**Figure 1**).

In a preliminary co-assembly, we co-assembled Pep-KG and TMP in a 1:1 charge ratio as a single Pep-KG strand has an overall charge of 1+ compared to the overall 3- charge of TMP. We observed that these Pep:TMP co-assemblies were able to mature into nanotubes within hours of being incubated at 37 °C. The secondary structure and the corresponding nano-structural morphology were examined by circular dichroism (CD) and transmission electron microscopy (TEM). After day 1, the co-assembly nanotubes disassembled into fibers which revealed that there are more underlying factors contributing to the stability of the co-assembled nanostructure.

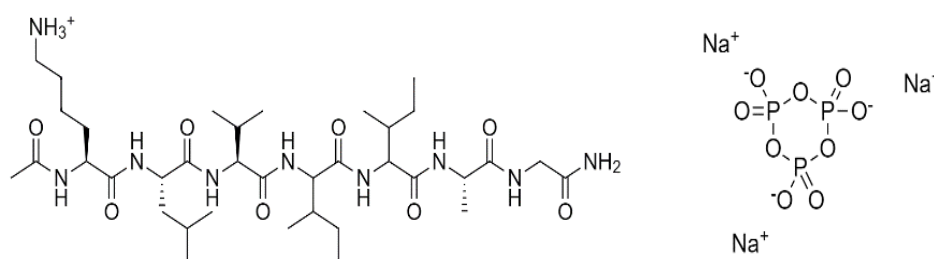


Figure 1. Structures of Pep-KG and Sodium Trimetaphosphate.

Pep-KG:TMP Co-assembly Structural Stability

We sought to determine the co-assembly's dependence on TMP concentration and its impact on the persistence length for nanotube structure. Along with the peptide-only assembly, two more co-assemblies were prepared by the addition of varying concentrations of TMP in which there was either a "limited" or "excess" amount of TMP in relation to charge-passivation to Pep-KG (**Figure 2**).

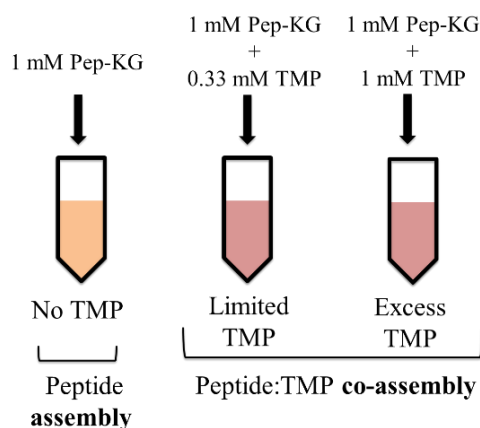


Figure 2. Pep-KG assembly and Pep-KG:TMP co-assembly concentrations. All solutions prepared in 40% acetonitrile solvent and incubated at 37 °C.

We followed the progression of secondary structure formation for all samples using CD. As expected, the Pep-KG assembly showed a classic β -sheet signature that formed between day 3 and 7 that persisted up to day 21 (**Figure 3**). Similarly, the limited and excess TMP co-assemblies showed a β -sheet signature that formed around the same time between 3 and 7 days (Figure 3). However, beyond these timepoints, the co-assemblies do not show a persisting β -sheet signature and instead, the peak for both limited and excess co-assemblies flattened out by day 14 and reappeared at the day 21 mark (**Figure 3b and 3c**).

To explore, the addition of fresh TMP in the no TMP assembly and the limited TMP co-assembly both exhibited a similar result that is a flattening of any visible signal which may indicate a structural change (**Figure 3**). While the assembly formed thin fibers and both limited and excess TMP co-assemblies formed nanotubes within hours (day 0), only the assembly structure persisted for over a

week (**Figure 4a.1-4a.2**). Addition of more TMP after noted disassembly resulted in the assembly's formation of particles, while the co-assembly is seemingly unaffected (**Figure 4a.3-4c.3**).

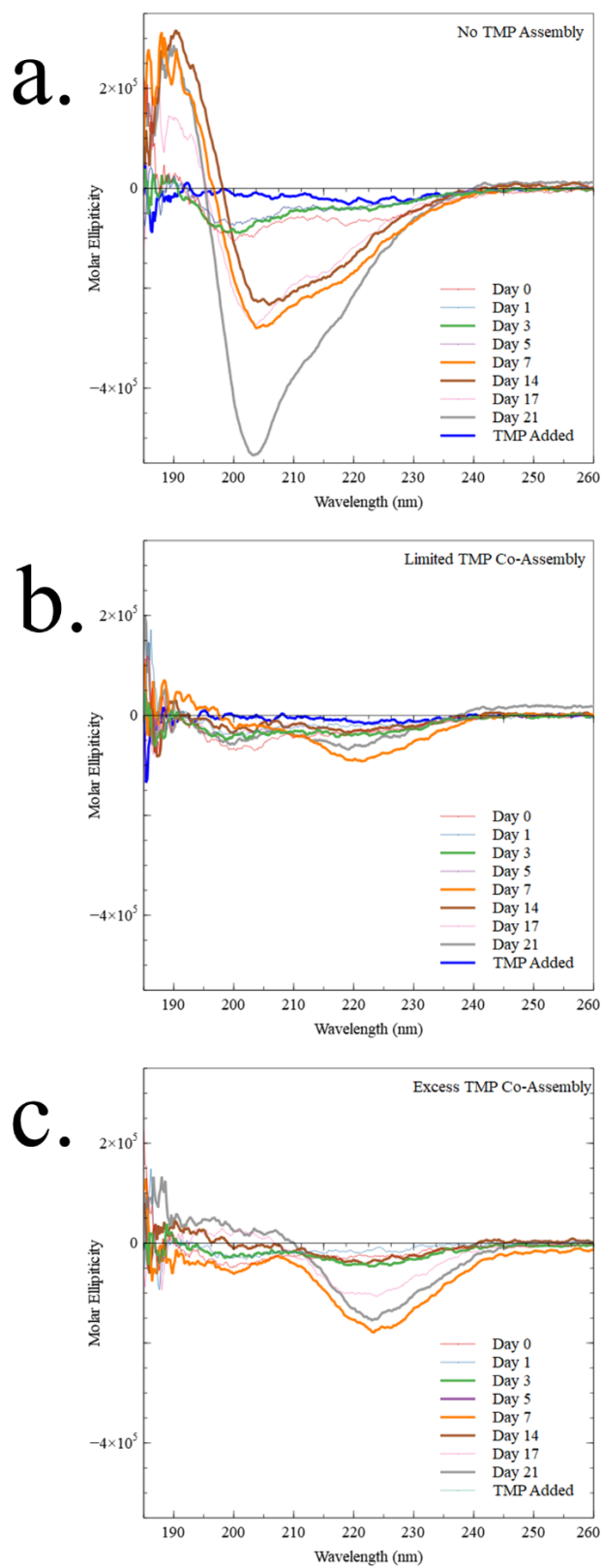


Figure 3. CD spectra of (a) No phosphate assembly (b) Limited phosphate co-assembly and (c) excess phosphate co-assembly from 0 days to 21 days at 37°C. The no phosphate and limited phosphate samples were treated with an addition of TMP after 21 days, the blue peak indicates 3 days after the addition.

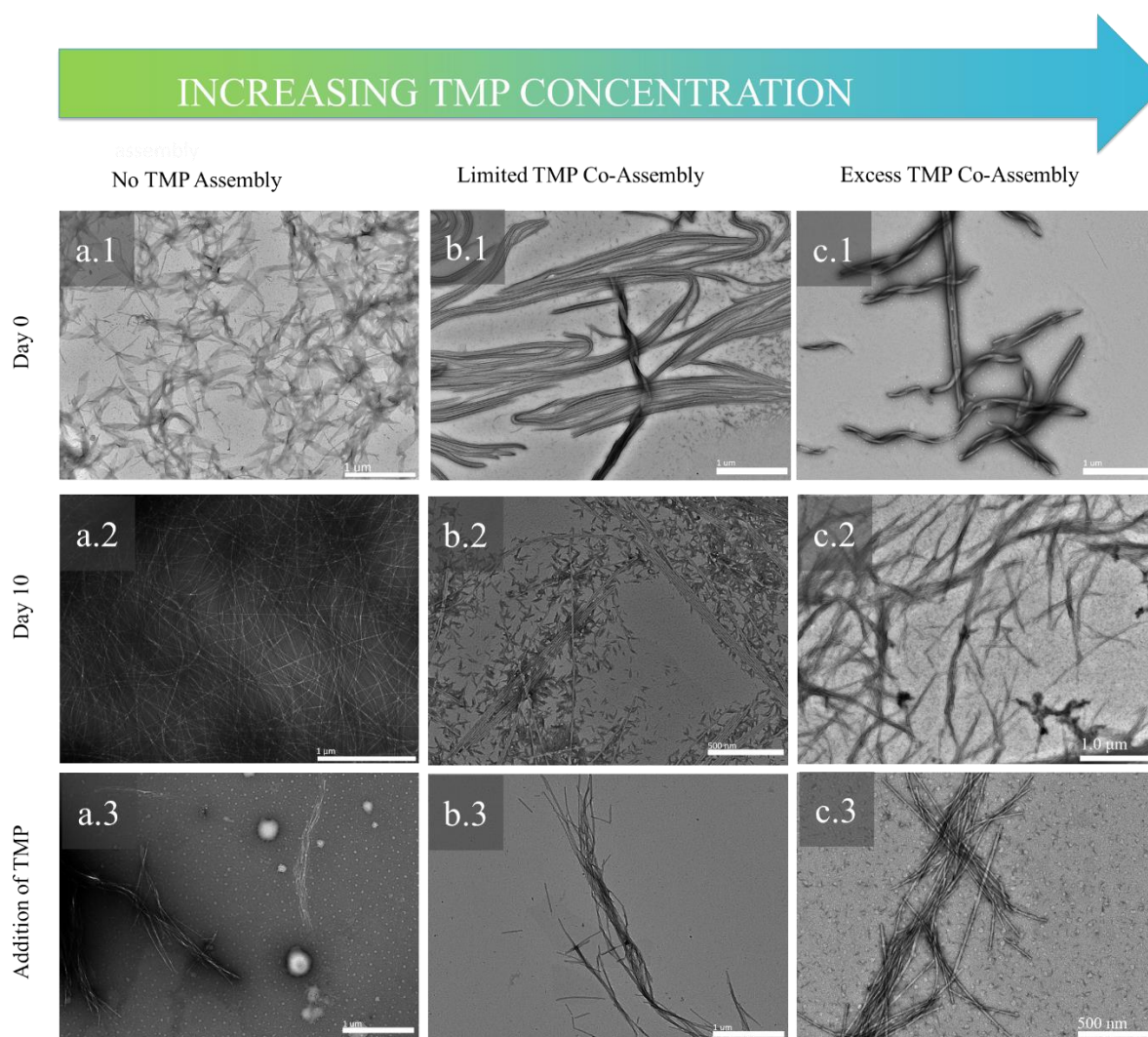


Figure 4. TEM images of assembly and the two co-assembled samples as noted in Figure 2.

Pep-KG:TMP- Salt Resistance and Ion Effects on Co-Assembly

Previous research showed that Pep-KG co-assembles with polymeric anions like RNA and Polyphosphate 50 to form structurally stable nanotubes that persist for days.¹⁴ Yet, the similar electrostatically stabilized Pep-KG:TMP co-assemblies, here, transition into ribbons and fibers from nanotubes only after 3 days, the structural stability of the co-assembled nanotubes must have altered.

Additionally, since more TMP was added to the co-assembly and there was no observable change which means that the added stability of more template molecules, so the conformational change is predicted to be due to another factor (**Figure 4a.3-4c.3**). This structural transition from nanotubes to fibers has been observed before when Pep-KG does not undergo a desalting protocol following purification.¹⁷ The results reported in the previous sections utilized Pep-KG that did not undergo a desalting protocol, leaving trace amounts of salts in the co-assembly from the synthesis and purification processes which can destabilize interactions between the lysine residue and phosphate electrostatics. Therefore, to further probe the question of how the residual salts compromises the structural stability of co-assembly nanotubes between Pep-KG and TMP, we prepared co-assembled desalted Pep-KG with TMP to compare to the previous non-salted co-assemblies.

The dominating interaction between the Pep-KG and TMP is expected to be electrostatics, according to our charge passivation model, thus it is expected that the effect of ionic strength will have critical impacts on coacervation formation and then, consequently on co-assembly. In addition, determining salt resistance, or the salt concentration above which no phase separation occurs can be probed easily through observation of secondary structure that would arise following coacervation. Since TMP is prepared as a salt of sodium trimetaphosphate so there is an excess of Na⁺ ions that may disrupt a balance of charges in solution, we chose to first identify the effects of NaCl on Pep-KG and TMP co-assemblies. The presence of Na⁺ and Cl⁻ ions is expected to have a screening effect on the charges of both Pep-KG and TMP which is proposed to disrupt formation of coacervates and thus LLPS at high salt concentration.

In the peptide-only assembly, as expected, the lack of the TMP template prevented any nanotubes from forming at day 0, and instead forming fibers which persisted through day 14 (**Figure 5a.1-5a.3**). At the low concentration of 0.33 mM NaCl, the nanotubes formed closely resemble that of the regular Pep-KG:TMP nanotubes (**Figure 5b.1-5b.3**). Beyond 0.33 mM NaCl, the nanotubes that were initially forming at day 0 for the 3 mM and 10 mM samples begin to unravel by day 4 and continue to persist at a sheet morphology up until the day 14 (**Figure 5d.1-5e.3**). In 20 mM NaCl solution, there were very little to no nanotubes forming on day zero in which the primary nanostructure are particles

and fibers, but by day 4 most of the nanostructures shown by TEM were particles (**Figure 5d.1-5e.3**). Despite being able to find that an increasing concentration of NaCl encouraged a morphology transition from nanotubes to fibers and ribbons, a small number of nanotubes were observed even in the 20 mM NaCl solution even though it was not representative of most of the sample (**Figure 5f.3**).

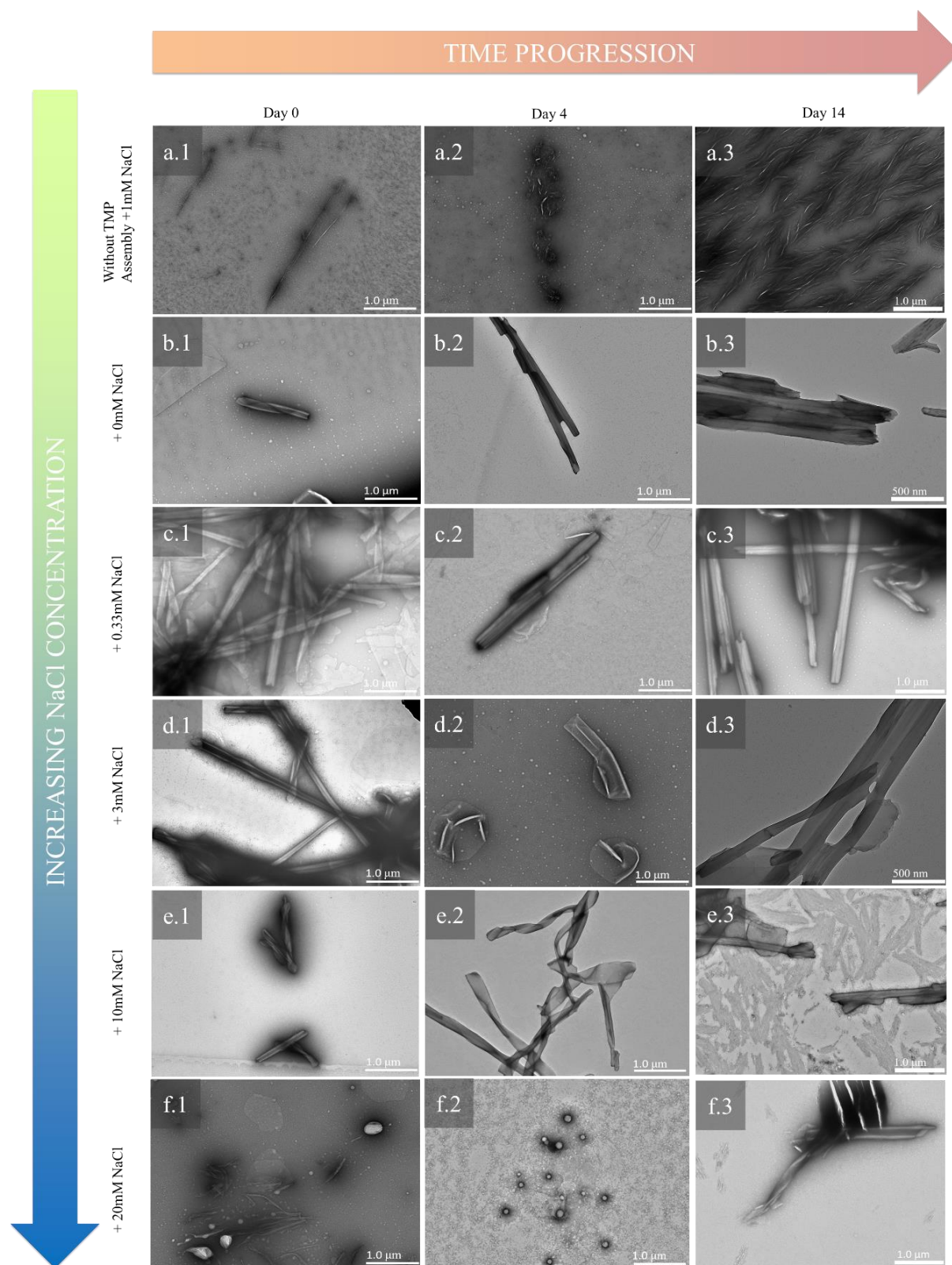


Figure 5. TEM images of Pep-KG assembly and the five co-assembled samples with increasing concentration of NaCl.

The ability of a series of salts to influence the solubility and stabilization of proteins in aqueous solution has already been studied and characterized by the Hofmeister series.^{2, 18} The order of the anion series follows from ions that facilitate stabilization of proteins to ones that facilitate unfolding: $\text{CO}_3^{2-} > \text{SO}_4^{2-} > \text{S}_2\text{O}_3^{2-} > \text{H}_2\text{PO}_4^- > \text{F}^- > \text{Cl}^- > \text{Br}^- > \text{NO}_3^- > \text{I}^- > \text{ClO}_4^- > \text{SCN}^-$.¹⁸ The iodide anion is reported to facilitate protein denaturation more than the chloride anion. As for the cation series, the ions are also ranked from most protein stabilizing to most destabilizing: $\text{N}(\text{CH}_3)_4^+ > \text{NH}_4^+ > \text{Cs}^+ > \text{Rb}^+ > \text{Na}^+ > \text{Li}^+ > \text{Ca}^{2+} > \text{Mg}^{2+} > \text{Zn}^{2+} > \text{Ba}^{2+}$.¹⁸ Therefore, the lithium cation tends to exhibit protein destabilization effects more than the sodium cation. Here we expect that as Pep-KG:TMP co-assemblies are incubated in NaI and LiCl solutions, the destabilizing interactions between the salt and the peptide cross- β assembly would further induce an observable conformational change in the co-assemblies' nanostructure.

At 0.33 mM of either NaCl or NaI, the NaCl treated co-assembly showed that nanotubes are more prevalent under TEM (**Figure 6a-6b**). At 10 mM solutions, the NaCl treated co-assembly shows thicker walled nanotubes compared to the ones of NaI (**Figure 6c-6d**). And at 275 mM NaI, co-assemblies primarily show sheet and ribbon morphology while in NaCl most of the nanostructures seen are sheets (**Figure 6e-6f**).

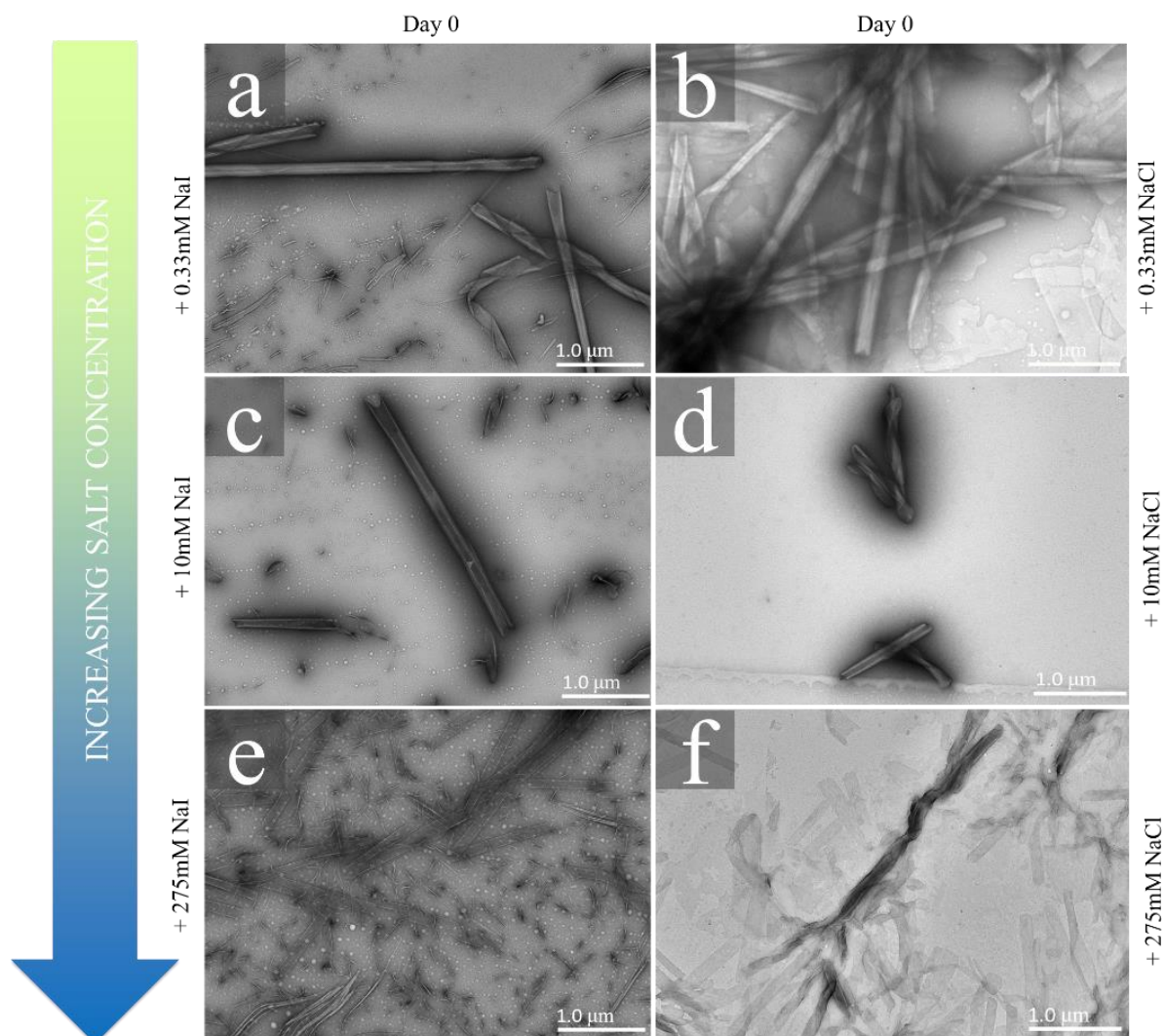


Figure 6. TEM images of Pep-KG:TMP co-assemblies with increasing concentration of NaI compared to NaCl.

The same trend in the nanotubes of quantity and wall thickness holds true for LiCl as it did for NaI (**Figure 7**). Overall, there are less nanotubes being formed when the Pep-KG:TMP co-assemblies are in LiCl than in NaCl (**Figure 7c-7d**). Also, the nanotubes are being formed tend to have thinner walls in LiCl than in NaCl.

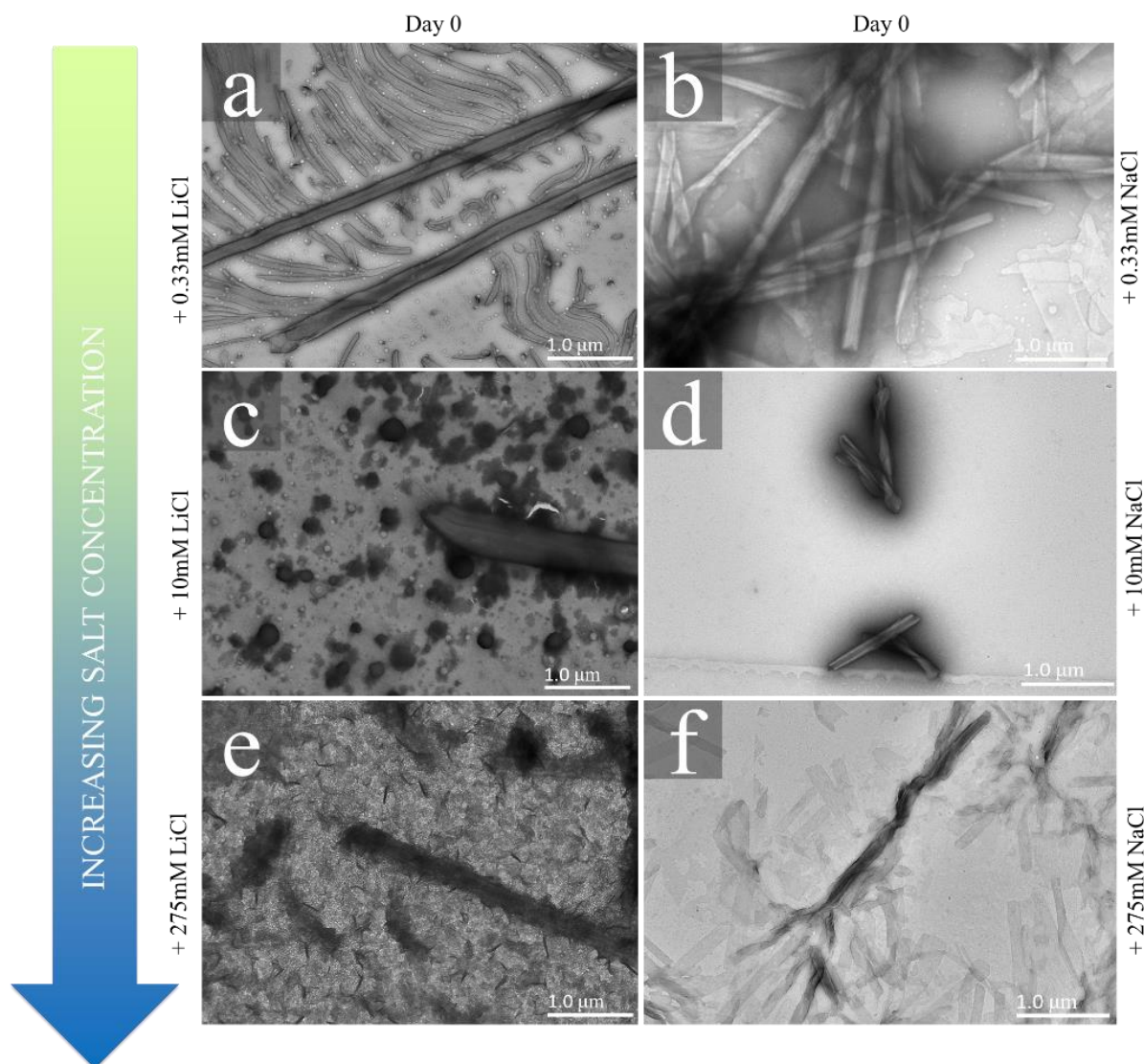


Figure 7. TEM images of Pep-KG:TMP co-assemblies with increasing concentration of LiCl compared to NaCl.

Although these results do align with the predictions of the Hofmeister salt series, the predictions of peptide stability based on salt effects is limited in this case as the system here includes an additional component, the phosphate template. Regardless, the impact of the destabilizing salts here coincides with previous research that showed that Pep-KG in MgCl_2 also formed thin-walled nanotubes with and without a stable nucleic acid template.¹⁹ So, it must be that the high salt concentration is the contributing variable to the wall thickness of the forms nanotubes rather than the phosphate template.

Pep-KG: DNA- Salt Effects on DNA Conformation

To gain insight into how the Hofmeister salt series impacts these peptide:phosphate co-assemblies, we decided to shift to a more well studied template like DNA specifically the Drew-Dickerson dodecamer sequence (CGCGAATTCGCG) which is known to reliably transition into the biologically relevant B-DNA form.²⁰ Previously, co-assemblies between Pep-KG and DNA both double-stranded DNA (dsDNA) versus single-stranded DNA (ssDNA) yielded the result that dsDNA is a more stable template for nanotubes when both co-assemblies are exposed to heat shock.¹⁷ Another measure of stability is resistance to salt conditions, thus to further probe template stability between dsDNA versus ssDNA, we can subject these co-assemblies to high salt conditions (NaCl and NaI). Therefore, the more stable DNA template, dsDNA versus ssDNA, would allow nanotubes to persist at higher concentrations of salt.

The thioflavin T (ThT) fluorescence assay is a well-known technique for the *in vitro* identification and quantification of β -sheet rich amyloid fibrils.²¹ ThT has enhanced and blue-shifted fluorescence, from 510 nm in its free state to 480 nm when bound, upon intercalating and constrained between the β -sheets.²¹ Across both the low and high NaCl and LiCl conditions, the Pep-KG:dsDNA co-assemblies tend to have a higher fluorescence intensity as compared to their Pep-KG:ssDNA counterparts (**Figure 8**). This finding suggests that dsDNA is a more stable template when co-assembling to Pep-KG as it is a more ordered and rigid polymer than ssDNA with two phosphate backbones shielding the hydrophobic bases. Upon closer analysis, the fluorescence difference between ssDNA and dsDNA co-assemblies is more pronounced at the lower salt concentrations rather than at the higher salt concentrations (**Figure 9**). This is a reflection of how increasing salt concentration maximizes charge screening up and IDP folding until a critical concentration. Past this threshold, however, increases in salt concentration causes disordered peptides to expand due to the electrostatic repulsion of the salt ions dominating and destabilizing the co-assembly architecture.⁵

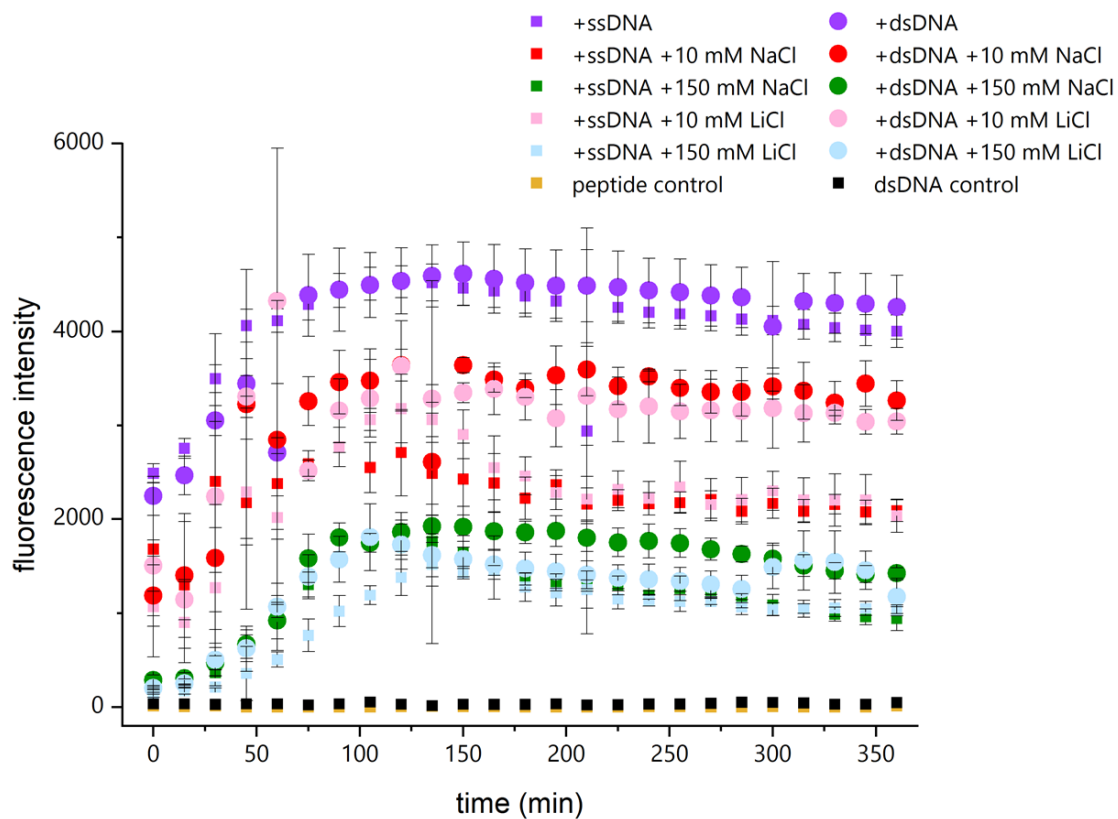


Figure 8. ThT assay comparing ssDNA and dsDNA template stability in NaCl and NaI conditions.

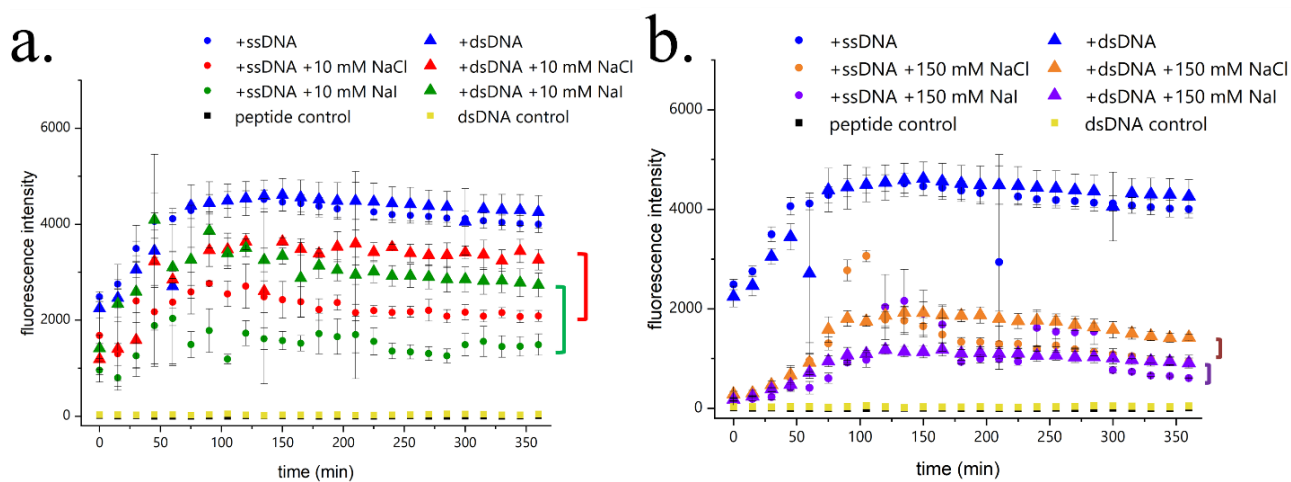


Figure 9. ThT assay showing ssDNA and dsDNA template stability difference is more apparent in a.) low [Na⁺] rather than b.) high [Na⁺] conditions.

Furthermore, the CD spectra reaffirms the point that dsDNA is a more stable template over time because ssDNA does not show β -sheet character at negative ellipticity of 220 nm at day 0 when dsDNA

does (Figure 10a & 10c). Interestingly, at the day 7 mark the amplitude of Pep-KG:dsDNA + 150mM LiCl β -sheet bands disappears while the NaCl assemblies retain the same intensity at 220 nm as from day 0 (Figure 10b & 10d). Molecular dynamics simulations predict that Li^+ and Na^+ interact with the DNA differently in less polarized solvents where Li^+ ions are most likely, among the alkali metals, to change the DNA conformation from B to A form.²² The strong interaction between Li^+ and the phosphate oxygen atoms restrains the electrostatic repulsion of the backbone while the coupling between Na^+ and the oxygen atoms is weaker.²² If a DNA conformational transition was observed, and the dsDNA + 150 mM LiCl co-assembly, the DNA structure would exist as a mixture of both the B and A forms. Thus, the CD spectra may be a result of the B and A DNA hybrid induced by high LiCl concentration, which would suggest that this hybrid could be a kinetically favorable template and explains its quick transition time but also lack of β -sheet persistence into day 7 (Figure 10b & 10d).

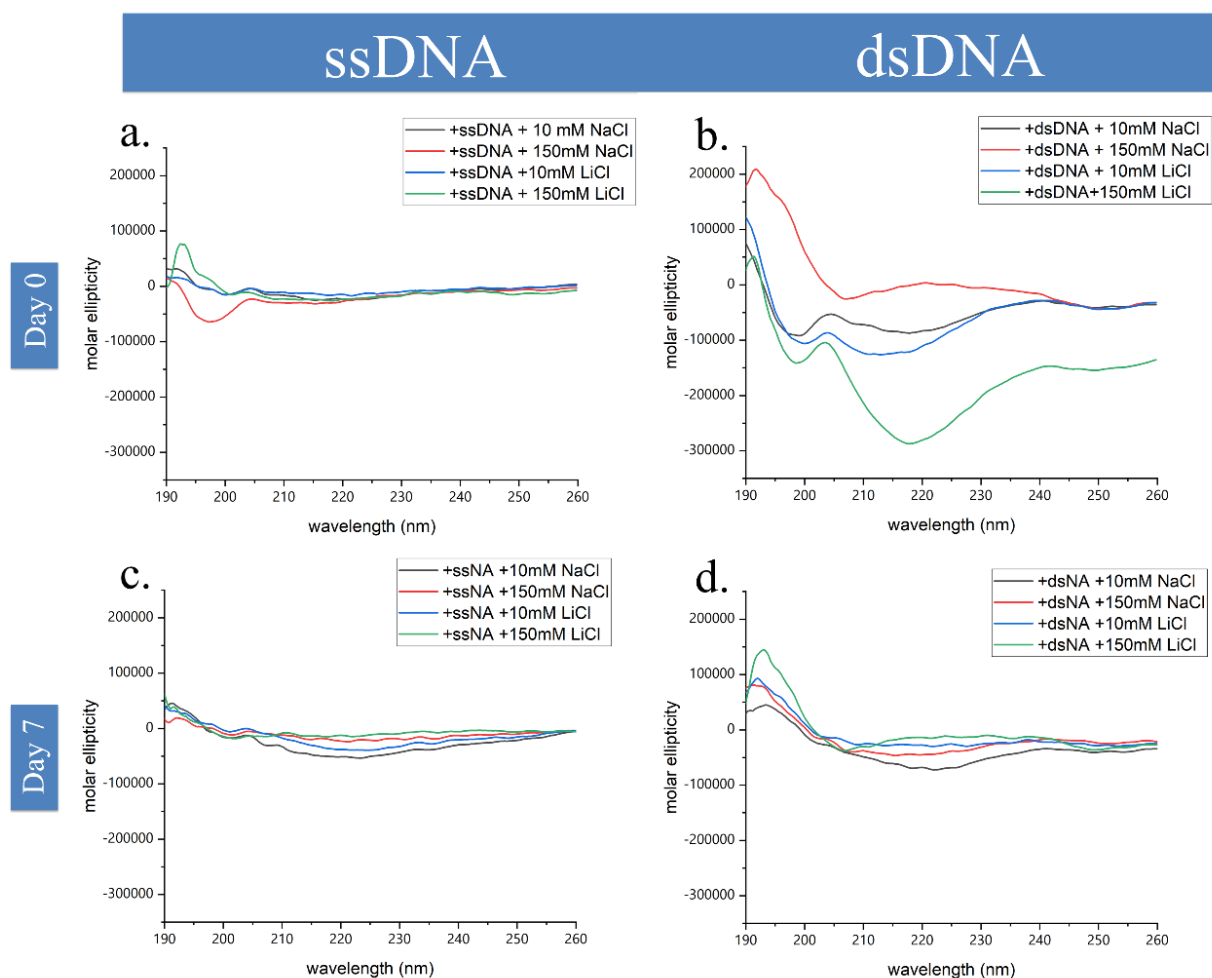


Figure 10. CD spectra of Pep-KG:ssDNA vs Pep-KG:dsDNA co-assemblies.

Conclusion

To extend the knowledge about the electrostatic complementarity between the previously studied peptide, Ac-KLVIIAG-NH₂, and other phosphate-based polymers studied the structural stability of co-assemblies in various salt conditions. Initially, the Pep-KG:TMP co-assemblies produce nanotubes that quickly transitioned into fibers and ribbons, but the desalted co-assemblies were able to persist longer as nanotubes according to TEM. This observation suggested that the residual ions in solution were able to alter the peptide and TMP electrostatics which warranted an investigation into the effects of NaCl concentration on co-assembly stability. With increasing NaCl concentration, the observed nanostructures of Pep-KG:TMP shifted from nanostructures to mainly particles by 20 mM NaCl treatment. Although we were able to observe a general qualitative trend, the exact mechanism for how either ion is interacting with either the peptide or TMP is unknown. A future direction can include a seeding experiment that would probe whether the rate of nucleation or propagation of the liquid-liquid phase separation is being impacted as they are critical steps into the formation of nanotubes. This seeding experiment would involve co-assembly of Pep-KG:TMP and then allowing for the maturation of nanotubes which then can be centrifuged down to create a nanotube rich pellet that can be seeded into prepared co-assemblies to monitor either the elongation of the existing nanotubes or the creation of more but shorter nanotubes. Furthermore, the comparison to other Hofmeister salts, NaI and LiCl, revealed that these destabilizing I⁻ and Li⁺ ions outcompete the phosphate templates in creating thin nanotube walls. Additionally, when co-assembling of Pep-KG with DNA double-stranded DNA is shown to be a more stable template than single-stranded DNA under the stress of high NaI and NaCl concentrations. Furthermore, we observed that Li⁺ may be capable of inducing a conformational DNA change from B to A form to create a kinetically stabilized β -sheet structure observable using the ThT fluorescence assay. Another future direction would be to monitor the DNA conformation of the co-assemblies via CD by extending the wavelength window to include DNA conformations that may be accessed (A, B and Z DNA forms). Overall the studies presented here have begun to extend our knowledge about salt effects not only on peptide stabilization but also in the novel context of peptide:phosphate co-assemblies.

Materials and Methods

Peptide synthesis and purification

Fmoc-protected amino acids, Rink amide resin, N,N'-diisopropylcarbodiimide (DIC), and OxymaPure were all purchased from Chem-Impex International, Inc. Rink amide resin was swollen in DMF for 5 minutes prior to synthesis, which was done using CEM Liberty Blue automatic peptide synthesizer. Each Fmoc-protected amino acid was dissolved at 0.2 M concentration for synthesis, and the instrument was set to produce 0.1 mmol peptide at a time.

Following synthesis, each peptide batch was washed and dried using dichloromethane via vacuum filtration. The dried resin was then exposed to a cleavage cocktail, to cleave the peptide from its solid support, containing 90% trifluoroacetic acid (TFA), 5% thioanisole, 3% 1,2-ethanedithiol, and 2% anisole in a 30 mL glass vial. The vial was then capped and shaken every 30 minutes or placed on an orbital shaker set to gently shake throughout the cleavage process, which was done at room temperature for 3 hours. At this point, the peptide should be separated from its solid support, and it was extracted using gravity filtration via a folded filter paper over cold ether in a 50 mL Corning conical tube. The peptide should flow through the filter paper and precipitate out of the ether. The leftover resin was washed with more TFA to quantitatively transfer as much peptide as possible. The ether solution was then centrifuged at 4000 rpm at 4°C for 15 minutes. After centrifugation, the supernatant was discarded, and the pellet was rinsed with more cold ether and vortexed. The centrifugation and cold ether-rinse steps were repeated twice more prior to overnight dessication of the cleaved peptide for HPLC purification.

The HPLC purification of each peptide involved dissolving the peptide in 40% MeCN and 0.1% TFA, and this solution was continuously sonicated using a bath sonicator. The HPLC was set to run on a gradient from 15 to 60% MeCN and 0.1% TFA at a rate of 20 mL/min and 1%/min. Pep-KG was found to elute at 31% MeCN, where its absorbance at 222 nm, indicative of the amide bond absorption, was highest. The product was confirmed by its molar mass using matrix-assisted laser desorption/ionization time-of-flight (MALDI-TOF) spectrometer. Following HPLC elution, the purified peptide solution was

rotovapped to rid of the organic solvent, flash frozen in liquid nitrogen, and then lyophilized for 48-72 hours, or until peptide is a light, white powder, at -72°C and 0.035 mbar.

Desalting peptides

HPLC-purified peptides were dissolved in 0.1% TFA in water. This solution was then run through Waters Sep-Pak C18 SPE cartridge and eluted using a solution of 50% MeCN and 0.1% TFA. The eluted peptide solution was then rotovapped to evaporate the organic solvent, followed by flash freezing via liquid nitrogen, and then lyophilized.

Peptide assembly and peptide:phosphate co-assemblies

All peptides used in assemblies and co-assemblies were the product of previously desalted and lyophilized peptides as described in the method above. The stock solution of 2 mM of Ac-KLVIIAG-NH₂, 10 mM sodium trimetaphosphate, and 600 mM NaCl were prepared separately in 40% acetonitrile. For the limited and excess TMP experiments, 1 mM of Pep-KG was the final concentration for all three conditions with the final limited TMP condition as 0.33 mM and the excess TMP concentration as 1 mM. For the NaCl concentration series, the final concentrations were 1 mM Pep-KG, 0.33 mM TMP and then 0, 0.33, 3, 10, 20 mM NaCl for the respective co-assemblies. For the salt control, the final concentrations were 1 mM Pep-KG and 1 mM NaCl. For the previously mentioned co-assemblies, the order of addition was 40% acetonitrile, salt solution, TMP, and finally Pep-KG.

The stock solutions of 1200mM NaI and 1200 LiCl were prepared in 100% water. For the NaI and LiCl series, the final concentrations were 1 mM Pep-KG, 0.33 mM TMP and then 0.33, 10, 275 mM NaI or LiCl for the respective co-assemblies. For the NaI and LiCl co-assemblies, the order of addition was 80% acetonitrile, 40% acetonitrile, salt solution in water, TMP, and finally Pep-KG to ensure the same concentration of solvent as the other co-assemblies.

Transmission electron microscopy (TEM)

8 μL of each sample was spotted upon 100-mesh copper-supported carbon TEM grids supplied by Electron Microscopy Services. The samples were left on each grid for 1 minute and then wicked using

cut up pieces of filter paper. 8 μ L of 2% uranyl acetate in water was then spotted on sample-spotted grids for negative staining, followed by wicking after 1 minute had elapsed. The grids were then imaged using a Hitachi HT-7700 transmission electron microscope, courtesy of the Robert Apkarian Electron Microscopy Core.

Circular dichroism (CD)

50 μ L of each sample was pipetted onto a Hellma 100-QS 0.1 mm path length quartz cuvette. The sample was analyzed using Jasco J-1500 CD spectrometer. Each CD spectra were baseline subtracted using the solvent, 40% MeCN, as the baseline. Subtracted spectra were then smoothed using the Jasco default smooth processing function.

Thioflavin T(ThT) fluorescence assay

Greiner Bio-One CellStar 96-well microplate was used to contain the samples for this ThT assay. In each sample well, of which had three replicates, the following were added: 1 μ L 10 mM ThT in 40% MeCN, 100 μ L 40% MeCN, and 74 μ L sample. The plate reader, BioTek Synergy MX, was set to 440 nm and 484 nm excitation and emission wavelengths, respectively, and to shake the microplate for 10 seconds prior to each reading. Each data set was composed of 25 total scans, with 15-minute intervals in between each scan.

References

1. Anfinsen, C. B., Principles that Govern the Folding of Protein Chains. *Science* **1973**, *181* (4096), 223-230.
2. Liu, Z.; Huang, Y., Advantages of proteins being disordered. *Protein Sci.* **2014**, *23* (5), 539-550.
3. Correll, C. C.; Bartek, J.; Dundr, M., The Nucleolus: A Multiphase Condensate Balancing Ribosome Synthesis and Translational Capacity in Health, Aging and Ribosomopathies. *Cells* **2019**, *8* (8), 869.
4. Shammas, S. L.; Travis, A. J.; Clarke, J., Remarkably Fast Coupled Folding and Binding of the Intrinsically Disordered Transactivation Domain of cMyb to CBP KIX. *The Journal of Physical Chemistry B* **2013**, *117* (42), 13346-13356.
5. Müller-Späh, S.; Soranno, A.; Hirschfeld, V.; Hofmann, H.; Rügger, S.; Reymond, L.; Nettels, D.; Schuler, B., Charge interactions can dominate the dimensions of intrinsically disordered proteins. *Proceedings of the National Academy of Sciences* **2010**, *107* (33), 14609-14614.
6. Madinya, J. J.; Chang, L.-W.; Perry, S. L.; Sing, C. E., Sequence-dependent self-coacervation in high charge-density polyampholytes. *Molecular Systems Design & Engineering* **2020**, *5* (3), 632-644.
7. Sing, C. E.; Perry, S. L., Recent progress in the science of complex coacervation. *Soft Matter* **2020**, *16* (12), 2885-2914.
8. Mitrea, D. M.; Cika, J. A.; Stanley, C. B.; Nourse, A.; Onuchic, P. L.; Banerjee, P. R.; Phillips, A. H.; Park, C.-G.; Deniz, A. A.; Kriwacki, R. W., Self-interaction of NPM1 modulates multiple mechanisms of liquid–liquid phase separation. *Nature Communications* **2018**, *9* (1), 842.
9. Uversky, V. N., Intrinsically disordered proteins in overcrowded milieu: Membrane-less organelles, phase separation, and intrinsic disorder. *Current Opinion in Structural Biology* **2017**, *44*, 18-30.
10. Posey, A. E.; Holehouse, A. S.; Pappu, R. V., Chapter One - Phase Separation of Intrinsically Disordered Proteins. In *Methods Enzymol.*, Rhoades, E., Ed. Academic Press: 2018; Vol. 611, pp 1-30.

11. Boeris, V.; Spelzini, D.; Salgado, J. P.; Picó, G.; Romanini, D.; Farruggia, B., Chymotrypsin–poly vinyl sulfonate interaction studied by dynamic light scattering and turbidimetric approaches. *Biochimica et Biophysica Acta (BBA) - General Subjects* **2008**, *1780* (9), 1032-1037.
12. Molliex, A.; Temirov, J.; Lee, J.; Coughlin, M.; Kanagaraj, Anderson P.; Kim, Hong J.; Mittag, T.; Taylor, J. P., Phase Separation by Low Complexity Domains Promotes Stress Granule Assembly and Drives Pathological Fibrillization. *Cell* **2015**, *163* (1), 123-133.
13. Wright, P. E.; Dyson, H. J., Linking folding and binding. *Current Opinion in Structural Biology* **2009**, *19* (1), 31-38.
14. Rha, A. K.; Das, D.; Taran, O.; Ke, Y.; Mehta, A. K.; Lynn, D. G., Electrostatic Complementarity Drives Amyloid/Nucleic Acid Co-Assembly. *Angew. Chem. Int. Ed.* **2020**, *59* (1), 358-363.
15. Mehta, A. K.; Lu, K.; Childers, W. S.; Liang, Y.; Dublin, S. N.; Dong, J.; Snyder, J. P.; Pingali, S. V.; Thiagarajan, P.; Lynn, D. G., Facial Symmetry in Protein Self-Assembly. *Journal of the American Chemical Society* **2008**, *130* (30), 9829-9835.
16. Rengifo, R. F.; Sementilli, A.; Kim, Y.; Liang, C.; Li, N. X. A.; Mehta, A. K.; Lynn, D. G., Liquid-Like Phases Preorder Peptides for Supramolecular Assembly. *ChemSystemsChem* **2020**, *n/a* (n/a).
17. Cato, M. L. *Nucleic Acid Secondary Structure Influences Properties of DNA/Peptide Co-Assemblies*; Emory University: 2018.
18. Kang, B.; Tang, H.; Zhao, Z.; Song, S., Hofmeister Series: Insights of Ion Specificity from Amphiphilic Assembly and Interface Property. *ACS Omega* **2020**, *5* (12), 6229-6239.
19. Rha, A. PhD Dissertation Emory University, 2016.
20. Kovaleva, N. A.; Strelnikov, I. A.; Zubova, E. A., Kinetics of the Conformational Transformation between B- and A-Forms in the Drew–Dickerson Dodecamer. *ACS Omega* **2020**, *5* (51), 32995-33006.
21. Hudson, S. A.; Ecroyd, H.; Kee, T. W.; Carver, J. A., The thioflavin T fluorescence assay for amyloid fibril detection can be biased by the presence of exogenous compounds. *The FEBS Journal* **2009**, *276* (20), 5960-5972.

22. Wen, J.; Shen, X.; Shen, H.; Zhang, F.-S., Hofmeister series and ionic effects of alkali metal ions on DNA conformation transition in normal and less polarised water solvent. *Mol. Phys.* **2014**, *112*, 2707.